Solar-Terrestrial Physics. 2026, vol. 12, iss. 2, pp. 109–113. DOI: 10.12737/stp-122202612. © 2026 D.A. Smirnov, V.F. Melnikov. Published by INFRA-M Academic Publishing House

DOI: 10.12737/stp-122202612
EDN: AHZUIW

Received November 14, 2025
Accepted March 03, 2026

POSSIBLE ERRORS IN RADIO SOURCE PARAMETERS RECOVERED BY THE FITTING METHOD RELATED TO ANISOTROPY OF THE ELECTRON DISTRIBUTION

D.A. Smirnov
Central Astronomical Observatory RAS at Pulkovo, Saint Petersburg, Russia, dmitriy.smirnov@unn.ru

V.F. Melnikov
Central Astronomical Observatory RAS at Pulkovo, Saint Petersburg, Russia, v.melnikov@gaoran.ru

Abstract. This paper examines errors in recovering (radio diagnostics) solar flare parameters (magnetic field, accelerated electron density, etc.) by fitting microwave spectra. The analysis was performed by diagnosing two model radio sources with known preset parameters, including given parameters of the pitch-angle anisotropy of emitting electrons. The diagnostics was carried out by a genetic minimization algorithm. It is shown that using the traditional approach on the assumption about isotropy of pitch angular distribution of electrons leads to significant systematic errors, in particular, to a strong underestimation of the magnetic field strength in the presence of longitudinal anisotropy of pitch angular distribution of electrons in a real radio source. When restoring the same parameters in view of possible anisotropy, the accuracy of the restoration increases markedly.

Keywords: solar flares, radioheliograph, radio diagnostics.

INTRODUCTION

Conducting research on solar flares with methods of radio diagnostics is extremely relevant, since only in the radio range it is possible to obtain detailed information on the coronal magnetic field and mildly relativistic electrons. The practical basis for this research has been provided by multifrequency radioheliographs developed in recent years, which can record frequency spectra of microwave emission in particular areas of a flare. First of all, these are regular observations carried out by the Siberian Radioheliograph (SRH) in frequency ranges 3–6, 6–12, and 12–24 GHz [Altyntsev et al., 2020] and by the solar-dedicated radio interferometer EOVSA (Expanded Owens Valley Solar Array) in the range 1–18 GHz [Gary et al., 2018; Chen et al., 2020]. In the next two years, it is also planned to start regular observations with the Chinese Spectroheliograph MUSER in the frequency range 2–15 GHz [Yan et al., 2021].

Diagnostics based on radioheliograph data is carried out by the fitting method, i.e. fitting observed frequency spectra from solar flare active regions to the theoretical ones, thereby recovering plasma and accelerated particle parameters. Previously, radio diagnostics with this approach was performed under the assumption of isotropic pitch-angle distribution of emitting nonthermal electrons [Morgachev et al., 2014; Fleishman et al., 2020]. The most interesting result of such microwave diagnostics is presented in [Fleishman et al., 2020, 2022], where the authors by analyzing September 10, 2017 solar flare from EOVSA data have revealed a decrease in the magnetic field in the region of the brightest microwave source. This allowed the authors to conclude that the rate of magnetic energy dissipation is high, which leads to the appearance of a super-Dreicer electric field, very efficient plasma heating, and particle acceleration. Similar rates of change of the magnetic field (dB/dt=1÷10 G/s) have recently been obtained during radio diagnostics of two solar flares (January 20, 2022 and July 16, 2023) from SRH observations [Smirnov, Melnikov, 2024].

Meanwhile, the pitch-angle distribution of electrons in a flare loop can in fact be anisotropic with both transverse [Melnikov et al., 2002] and longitudinal anisotropy [Morgachev et al., 2014, 2015; Shain et al., 2017]. Moreover, the plasma and accelerated particle parameters at the loop apex can sometimes be recovered only if the pitch-angle distribution of energetic electrons is anisotropic (longitudinal), and there is no solution for the isotropic distribution [Morgachev et al., 2014].

This fact must be considered during diagnostics, by introducing additional unknown parameters into the fitting procedure. This significantly complicates the recovery procedure, since the number of selected parameters and hence the equations necessary to find them increases. On the other hand, it is now becoming possible due to the development of new multifrequency radio interferometers: SRH, MUSER, and EOVSA.

The amount of computing resources needed to solve this problem should also be kept in mind. As is known, for sufficient sampling in the multidimensional parameter space it is necessary to account for the number of points (in this case, sets of plasma characteristics), which increases significantly with dimension. In particular, for the space of dimension n (n is the number of desired parameters) about k^n points is required, where k is the number of points necessary to completely fill one dimension within the formulated problem.

The purpose of this work is to find possible errors in estimating the magnetic field and parameters of accelerated electrons under the assumption of both isotropic and anisotropic electron distributions, as well as to compare their values to determine the degree of accuracy of each approach.

1. DESCRIPTION OF MODELS EMPLOYED

The analysis has been carried out using two model radio sources with different preset parameters (Table 1).

The following conditions have been selected. The electron energy spectrum was defined as a double power law electron spectrum with a break at energy E_{break}, i.e. consisting of two parts ($E<E_{break}$, $E>E_{break}$), where both the high-energy and low-energy parts were described by power laws with different spectral indices δ_1 and δ_2. Minimum and maximum limits in electron energy distributions E_{min}=30 keV and E_{max}=10 MeV.

The analyzed uniform regions of the model sources had the same depth $D=3\cdot10^8$ cm, area $S=2.76\cdot10^{17}$ cm^2, and background plasma temperature $T=10^7$ K. Nonetheless, other parameters (background plasma electron density n_0, magnetic field strength B, angle between the magnetic field direction and the line of sight θ, double-power-law break energy E_{break}, and spectral indices δ_1 and δ_2) differ in the models (see Table 1). At the same time, in model No. 2 the ratio of the plasma electron density to the magnetic field strength is increased 8.75 times, as compared to model No. 1, to enhance the Razin effect to a level at which the gyrosynchrotron radiation flux density changes it causes significantly exceed instrumental measurement errors. This provides a means for performing radio diagnostics of background plasma density.

The pitch-angle distribution of electrons was defined as anisotropic in the form of a Gaussian beam:

$$g(\mu) = A\exp\left[-\frac{(\mu-\mu_0)^2}{\mu_1^2}\right], \qquad (1)$$

where $\mu_0=\cos_0$, α_0 is the angle between the electron velocity direction at maximum pitch-angle distribution and the magnetic field. The pitch angle α_0 was taken to be 0° (longitudinal anisotropy), 30° and 90° (transverse anisotropy). μ_1 characterizing the beam width was assumed to be 0.2. As the values increase to $\mu_1 \approx 1$ or more, the distribution becomes almost isotropic (Figure 1). The frequency spectra of gyrosynchrotron emission from the model sources, which were calculated for different α_0 values of the anisotropic pitch-angle distribution (μ_1=0.2), are shown in Figures 2–4.

2. RESULTS OF NUMERICAL EXPERIMENTS

Table 2 presents relative deviations of recovered values from those given for each of the two radio source models. Deviations of large parameters, such as n_0, n_b, B, were calculated by the formula

$$\delta=(A_r-A_m)/A_m\cdot 100\ \% \qquad (2)$$

where A_r is the recovered parameter; A_m is the model parameter. Deviations of other parameters (θ, E_{break}, δ_1, δ_2, α_0, μ_1) were given in units of measurement of these parameters and calculated using the formula $\Delta A=A_r-A_m$. It follows from Table 2 that the errors in results of diagnostics of the parameters were determined under the assumption of both isotropic distribution of nonthermal electrons and a number of anisotropic distributions (α_0=0°, 30°, 90°).

For each of the two radio source models, comparison between deviations of the recovered parameters from the preset ones shows that consideration of anisotropy made it possible to significantly improve the accuracy in recovering the parameters of the model radio sources. This is especially true for the following parameters:

1) magnetic field strength;
2) angle between magnetic field lines and the line of sight;
3) accelerated electron density;
4) double-power-law break energy.

A noticeable improvement in the accuracy of the recovery also takes place for the electron energy spectrum parameters δ_1 and δ_2. Note that the parameter μ_1 (beam width) for both models and all values of α_0 during diagnostics in view of possible anisotropy demonstrated high recovery accuracy.

At the same time, there is a tendency to increase the error in some parameters at small α_0 when recovering spectra under the assumption of isotropy. In particular, the strongest deviations from the true value are shown by the recovered plasma density n_0 (deviation increase to 99 %) and magnetic field B (deviation increase to 90.3 %).

Particular attention should be given to the error in recovering the magnetic field strength at different α_0. Tables indicate that during diagnostics under the assumption about isotropy of emitting electrons as α_0 decreases, i.e. the degree of longitudinal anisotropy in the radio source increases as does the error in recovering B. In this case, the deviation sign of the recovered value turns out to be negative (B decreases).

Table 1

Parameters of model radio sources

No.	n_0, cm^{-3}	B, G	θ, deg	$n_b(E>0.1$ Mev), cm^{-3}	E_{break}, Mev	δ_1	δ_2	α_0		
Model No. 1	1e10	350	85	2.2e5	0.3	4	8	0	30	90
Model No. 2	5e10	200	65	7.2e5	0.5	3	5			

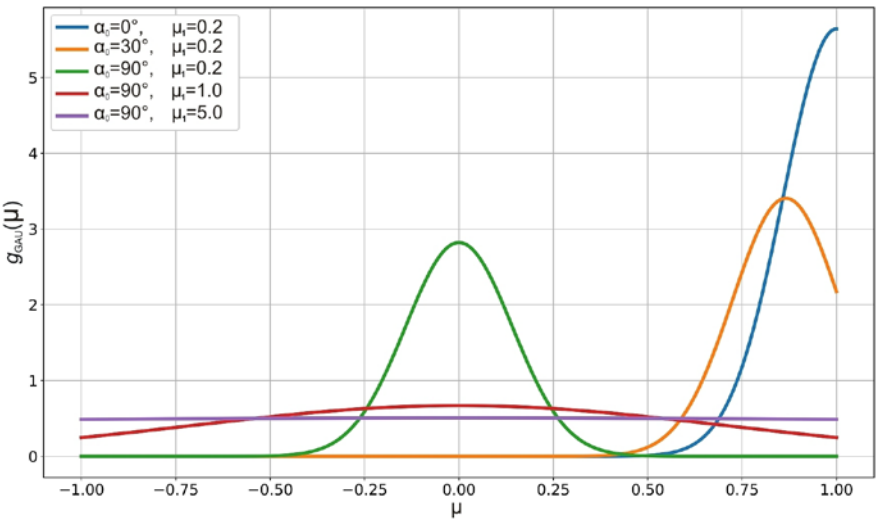

Figure 1. Pitch-angle electron distribution at different α_0 and μ_1

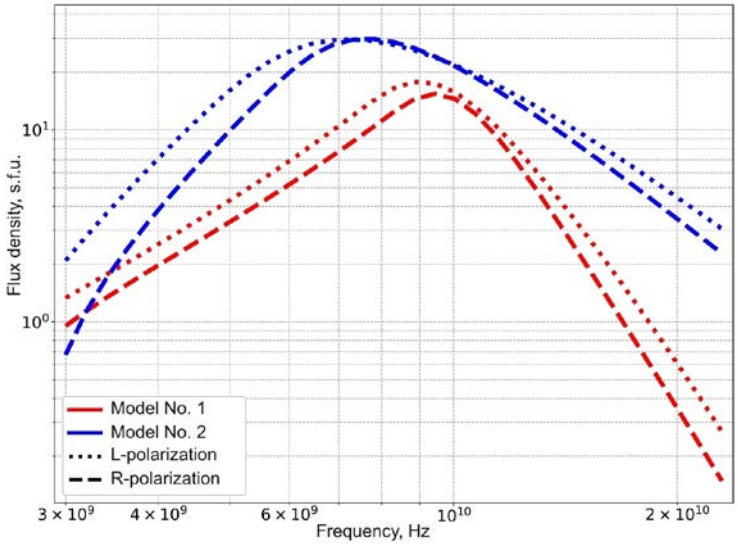

Figure 2. Frequency spectra of gyrosynchrotron emission in the model radio sources under study at α_0=0°

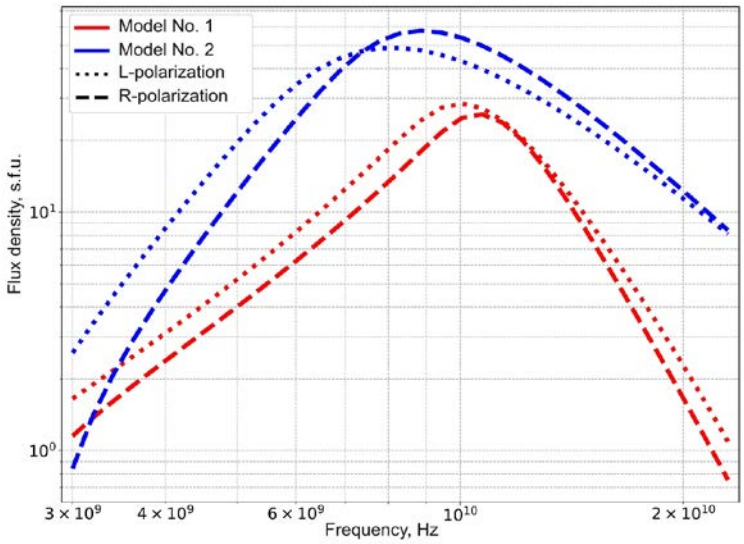

Figure 3. Frequency spectra of gyrosynchrotron emission in the model radio sources of interest at α_0=30°

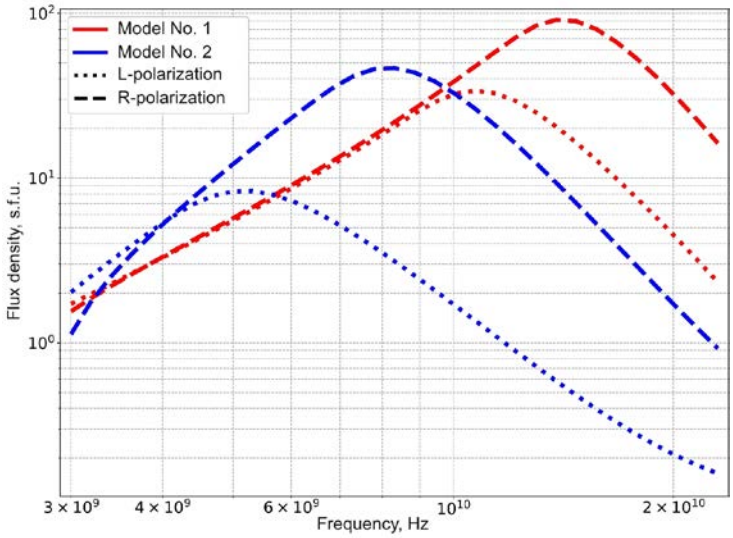

Figure 4. Frequency spectra of gyrosynchrotron emission in the model radio sources of interest at α_0=90°

Table 2

Radio source model employed	Approximation in use	Model value α_0	$\Delta n_0/n_{0m}$, %	$\Delta B/B_m$, %	$\Delta\theta$, deg	$\Delta n_b/n_{bm}$, %	ΔE_{break}, Mev	$\Delta\delta_1$	$\Delta\delta_2$	$\Delta\alpha_0$, deg	$\Delta\mu_1$
Model No. 1	isotropic	0°	–98.0	–90.3	+55.0	+372283	+0.4	–0.5	+3.0	–	–
		30°	–89.7	–75.1	–36.4	+881898	–0.3	–3.0	+1.7	–	–
		90°	–35.7	+0.9	–30.3	+1569.1	–0.1	+0.8	+1.5	–	–
	anisotropic	0°	–13.8	–9.2	–1.6	+117.8	+0.4	+0.4	+32.2	+22.1	–0.03
		30°	+4.1	+3.7	+8.4	–25.1	- 0.02	–0.1	–0.07	–1.1	+0.01
		90°	+2.11	+5.24	+3.9	+91.2	+0.02	–0.4	+1.7	+22.9	+0.2
Model No. 2	isotropic	0°	–99.0	–40.7	+40.9	+2133	–0.04	+2.2	–2.8	–	–
		30°	∞	–34.4	+42.3	+1520	–0.2	+1.1	–2.3	–	–
		90°	+10.8	+8.3	–25.3	+185.2	+0.09	+0.2	+15.6	–	–
	anisotropic	0°	+0.09	–0.02	–0.0003	–0.02	+0.002	+0.002	+0.09	+1.8	–0.00007
		30°	∞	+3.8	–2.0	–2.7	+0.03	–0.1	+3.3	–14.1	+0.02
		90°	+2.7	–0.1	+0.3	+1.3	–0.03	–0.006	–1	+0.3	+0.0002

Thus, a decrease in the degree of transverse anisotropy in a radio source and an increase in the degree of longitudinal anisotropy can be interpreted during diagnostics under the assumption of isotropy of emitting electrons as a decrease in the magnetic field strength, although in reality this will not be the case. This phenomenon may be one of the reasons for the decrease in the recovered magnetic field [Fleishman et al., 2020, 2022; Smirnov, Melnikov, 2024] during flares whose diagnostics was carried out precisely under the assumption of isotropy, without considering the possible longitudinal anisotropy of the pitch-angle distribution of emitting electrons.

CONCLUSION

The numerical simulation and subsequent fitting of gyrosynchrotron emission spectra clearly demonstrate that ignoring the possible anisotropy of the pitch-angle distribution of nonthermal electrons leads to systematic and significant errors in diagnosing key parameters of radio sources in solar active regions. Using the anisotropy-based approach is not just preferable, but a prerequisite for obtaining reliable results.

The work was financially supported by RSF (grant No. 22-12-00308–P). We are grateful to the team of the Siberian Radioheliograph for access to the data on the flares recorded by SRH, as well as for all possible assistance in processing the data and friendly support in carrying out this work.

REFERENCES

Altyntsev A.T., Lesovoi S.V., Globa M.V., et al. Multiwave Siberian Radioheliograph. *Sol.-Terr. Phys.* 2020, vol. 6, iss. 2, pp. 30–40. https://doi.org/10.12737/stp-62202003.

Chen B., Yu S., Reeves K.K., Gary D.E. Microwave spectral imaging of an erupting magnetic flux rope: Implications for the standard solar flare model in three dimensions. *Astrophys. J. Lett.* 2020, vol. 895, p. L50. https://doi.org/10.3847/2041-8213/ab901a.

Fleishman G.D., Gary D.E., Chen B., et al. Decay of the coronal magnetic field can release sufficient energy to power a solar flare. *Science*. 2020, vol. 367, iss. 6475, pp. 278–280. https://doi.org/10.1126/science.aax6874.

Fleishman G.D., Nita G.M., Chen B., et al. Solar flare accelerates nearly all electrons in a large coronal volume. *Nature*. 2022, vol. 606, pp. 674–677. https://doi.org/10.1038/s41586-022-04728-8.

Gary D.E., Chen B., Dennis B.R., et al. Microwave and hard X-ray observations of the 2017 September 10 solar limb flare. *Astrophys. J.* 2018, vol. 863, no. 1, 9 p. https://doi.org/10.3847/1538-4357/aad0ef.

Melnikov V.F., Shibasaki K., Reznikova V.E. Loop top nonthermal microwave source in extended solar flaring loops. *Astrophys. J. Lett.* 2002, vol. 580, pp. 185–188.

Morgachev A.S., Kuznetsov S.A., Melnikov V.F. Radio diagnostics of the solar flaring loop parameters by direct fitting method. *Geomagnetism and Aeronomy.* 2014, vol. 54, iss. 7, pp. 933–942. https://doi.org/10.1134/S0016793214070081.

Morgachev A.S., Kuznetsov S.A., Melnikov V.F., Simoes J.A. Modeling the distribution of circular polarization degree of solar flare loops in event 19 July 2012. *Geomagnetism and Aeronomy.* 2015, vol. 55, iss. 8, pp. 1118–1123. https://doi.org/10.1134/S0016793215080228.

Shain A.V., Melnikov V.F., Morgachev A.S. The role of quasi-transverse propagation in observed polarization of flare loop microwave radiation. *Geomagnetism and Aeronomy.* 2017, vol. 57, pp. 988–995. https://doi.org/10.1134/S0016793217080217.

Smirnov D.A., Melnikov V.F. Microwave diagnostics of flare plasma by the direct fitting method based on data from the Siberian Radioheliograph. *Sol.-Terr. Phys.* 2024, vol. 10, iss. 3, pp. 25–36. https://doi.org/10.12737/stp-103202404.

Yan Y., Chen Z., Wang W., et al. Mingantu spectral radioheliograph for solar and space weather studies. *Frontiers in Astronomy and Space Sciences*. 2021, vol. 8, 584043. https://doi.org/10.3389/fspas.2021.584043.

Original Russian version: Smirnov D.A., Melnikov V.F., published in Solnechno-zemnaya fizika. 2026, vol. 12, no. 2, pp. 119–123. https://doi.org/10.12737/szf-122202612.

How to cite this article:

Smirnov D.A., Melnikov V.F. Possible errors in radio source parameters recovered by the fitting method related to anisotropy of the electron distribution. *Sol.-Terr. Phys.* 2026, vol. 12, iss. 2, pp. 109–113. https://doi.org/10.12737/stp-122202612.